

Optimal Variance Control of the Score Function Gradient Estimator for Importance Weighted Bounds

Valentin Liévin¹ Andrea Dittadi¹ Anders Christensen¹ Ole Winther^{1, 2, 3}

¹ Section for Cognitive Systems, Technical University of Denmark

² Bioinformatics Centre, Department of Biology, University of Copenhagen

³ Centre for Genomic Medicine, Rigshospitalet, Copenhagen University Hospital
 {valv, adit}@dtu.dk, anders.christensen321@gmail.com, olwi@dtu.dk

Abstract

This paper introduces novel results for the score function gradient estimator of the importance weighted variational bound (IWAE). We prove that in the limit of large K (number of importance samples) one can choose the control variate such that the Signal-to-Noise ratio (SNR) of the estimator grows as \sqrt{K} . This is in contrast to the standard pathwise gradient estimator where the SNR decreases as $1/\sqrt{K}$. Based on our theoretical findings we develop a novel control variate that extends on VIMCO. Empirically, for the training of both continuous and discrete generative models, the proposed method yields superior variance reduction, resulting in an SNR for IWAE that increases with K without relying on the reparameterization trick. The novel estimator is competitive with state-of-the-art reparameterization-free gradient estimators such as Reweighted Wake-Sleep (RWS) and the thermodynamic variational objective (TVO) when training generative models.

1 Introduction

Gradient-based learning is now widespread in the field of machine learning, in which recent advances have mostly relied on the backpropagation algorithm, the workhorse of modern deep learning. In many instances, for example in the context of unsupervised learning, it is desirable to make models more expressive by introducing stochastic latent variables. Backpropagation thus has to be augmented with methodologies for marginalization over latent variables.

Variational inference using an inference model (amortized inference) has emerged as a key method for training and inference in latent variable models [1–7]. The pathwise gradient estimator, based on the reparameterization trick [2, 3], often gives low-variance estimates of the gradient for continuous distributions. However, since discrete distributions cannot be reparameterized, these methods are not applicable to inference in complex simulators with discrete variables, such as reinforcement learning or advanced generative processes [8–11]. While the score function (or Reinforce) estimator [12] is more generally applicable, it is well known to suffer from large variance. Consequently, most of the recent developments focus on reducing the variance using control variates [13–18] and using alternative variational objectives [9, 19–21].

Recently, variational objectives tighter than the traditional evidence lower bound (ELBO) have been proposed [21, 22]. In importance weighted autoencoders (IWAE) [22] the tighter bound comes with the price of a K -fold increase in the required number of samples from the inference network. Despite yielding a tighter bound, using more samples can be detrimental to the learning of the inference model [23]. In fact, the Signal-to-Noise ratio (the ratio of the expected gradient to its standard deviation) of the pathwise estimator has been shown to decrease at a rate $\mathcal{O}(K^{-1/2})$ [23]. Although this can be improved to $\mathcal{O}(K^{1/2})$ by exploiting properties of the gradient to cancel high-variance

terms [24], the variational distributions are still required to be reparameterizable. In this work we introduce OVIS (*Optimal Variance – Importance Sampling*), a novel score function-based estimator for importance weighted objectives with improved SNR.

The main contributions of this paper are: 1) A proof that, with an appropriate choice of control variate, the score function estimator for the IWAE objective can achieve a Signal-to-Noise Ratio $\text{SNR} = \mathcal{O}(K^{1/2})$ as the number of importance samples $K \rightarrow \infty$. 2) A derivation of OVIS, a class of practical low-variance score function estimators following the principles of our theoretical analysis. 3) State-of-the-art results on a number of non-trivial benchmarks for both discrete and continuous stochastic variables, with comparison to a range of recently proposed score function methods.

2 Optimizing the Importance Weighted Bound

Importance weighted bound (IWAE) Amortized variational inference allows fitting a latent variable model $p_\theta(\mathbf{x}, \mathbf{z})$ to the data using an approximate posterior $q_\phi(\mathbf{z}|\mathbf{x})$ [2]. By using multiple importance weighted samples, we can derive a lower bound to the log marginal likelihood that is uniformly tighter as the number of samples, K , increases [22]. The *importance weighted bound* (IWAE) for one data point \mathbf{x} is:

$$\mathcal{L}_K(\mathbf{x}) := \mathbb{E} [\log \hat{Z}] \quad \hat{Z} := \frac{1}{K} \sum_{k=1}^K w_k \quad w_k := \frac{p_\theta(\mathbf{x}, \mathbf{z}_k)}{q_\phi(\mathbf{z}_k|\mathbf{x})}, \quad (1)$$

where \mathbb{E} denotes an expectation over the K -copy variational posterior $q_\phi(\mathbf{z}_{1:K}|\mathbf{x}) := \prod_{k=1}^K q_\phi(\mathbf{z}_k|\mathbf{x})$. This bound coincides with the traditional evidence lower bound (ELBO) for $K = 1$. The log likelihood lower bound for the entire data set is $\mathcal{L}_K(\mathbf{x}_{1:n}) = \sum_{i=1}^n \mathcal{L}_K(\mathbf{x}_i)$. In the following we will derive results for one term $\mathcal{L}_K = \mathcal{L}_K(\mathbf{x})$.

Score function estimator Without making assumptions about the variational distribution, the gradient of the importance weighted bound (1) with respect to the parameters of the approximate posterior factorizes as (see Appendix A):

$$\nabla_\phi \mathcal{L}_K = \mathbb{E} \left[\sum_k d_k \mathbf{h}_k \right] \quad d_k := \log \hat{Z} - v_k \quad v_k := \frac{w_k}{\sum_{l=1}^K w_l}, \quad (2)$$

where $\mathbf{h}_k := \nabla_\phi \log q_\phi(\mathbf{z}_k|\mathbf{x})$ is the score function. A Monte Carlo estimate of the expectation in (2) yields the *score function* (or *Reinforce*) *estimator*.

Control variates The vanilla score function estimator of (2) is often not useful in practice due to its large sample-to-sample variance. By introducing control variates that aim to cancel out zero expectation terms, this variance can be reduced while keeping the estimator unbiased.

Given posterior samples $\mathbf{z}_1, \dots, \mathbf{z}_K \sim q_\phi(\mathbf{z}_{1:K}|\mathbf{x})$, let \mathbf{z}_{-k} denote $[\mathbf{z}_1, \dots, \mathbf{z}_{k-1}, \mathbf{z}_{k+1}, \dots, \mathbf{z}_K]$, let $\mathbb{E}_k[\dots]$ and $\mathbb{E}_{-k}[\dots]$ be the expectations over the variational distributions of \mathbf{z}_k and \mathbf{z}_{-k} , respectively, and let $\{c_k\}_{k=1}^K$ be scalar control variates, with each $c_k = c_k(\mathbf{z}_{-k})$ independent of \mathbf{z}_k . Using the independence of c_k and \mathbf{h}_k for each k , and the fact that the score function has zero expectation, we have $\mathbb{E}[c_k \mathbf{h}_k] = \mathbb{E}_{-k}[c_k] \mathbb{E}_k[\mathbf{h}_k] = 0$. Thus, we can define an unbiased estimator of (2) as:

$$\mathbf{g} := \sum_k (d_k - c_k) \mathbf{h}_k \quad (3)$$

$$\mathbb{E}[\mathbf{g}] = \mathbb{E} \left[\sum_k (d_k - c_k) \mathbf{h}_k \right] = \mathbb{E} \left[\sum_k d_k \mathbf{h}_k \right] = \nabla_\phi \mathcal{L}_K. \quad (4)$$

In the remainder of this paper, we will use the decomposition $d_k = f_k + f_{-k}$, where $f_k = f_k(\mathbf{z}_k, \mathbf{z}_{-k})$ and $f_{-k} = f_{-k}(\mathbf{z}_{-k})$ denote terms that depend and do not depend on \mathbf{z}_k , respectively. This will allow us to exploit the mutual independence of $\{\mathbf{z}_k\}_{k=1}^K$ to derive optimal control variates.

Signal-to-Noise Ratio (SNR) We will compare the different estimators on the basis of their Signal-to-noise ratio. Following [23], we define the SNR for each component of the gradient vector as

$$\text{SNR}_i := \frac{|\mathbb{E}[g_i]|}{\sqrt{\text{Var}[g_i]}}, \quad (5)$$

where g_i denotes the i th component of the gradient vector.

In Section 3 we derive the theoretical SNR for the optimal choice of control variates in the limit $K \rightarrow \infty$. In Section 4 we derive the optimal scalar control variates $\{c_k\}_{k=1}^K$ by optimizing the trace of the covariance of the gradient estimator \mathbf{g} , and in Section 6 we experimentally compare our approach with state-of-the-art gradient estimators in terms of SNR.

3 Asymptotic Analysis of the Signal-to-Noise Ratio

Assuming the importance weights have finite variance, i.e. $\text{Var}[w_k] < \infty$, we can derive the asymptotic behavior of the SNR as $K \rightarrow \infty$ by expanding $\log \hat{Z}$ as a Taylor series around Z [23]. A direct application of the pathwise gradient estimator (reparameterization trick) to the importance weighted bound results in an SNR that scales as $\mathcal{O}(K^{-1/2})$ [23], which can be improved to $\mathcal{O}(K^{1/2})$ by exploiting properties of the gradient [24]. In the following we will show that, for a specific choice of control variate, the SNR of the score function estimator scales as $\mathcal{O}(K^{1/2})$. It is therefore possible to define a score function estimator for which *increasing the number of importance samples is beneficial to gradient updates of the parameters of the variational distribution*.

For the asymptotic analysis we rewrite the estimator as $\mathbf{g} = \sum_k (-\frac{\partial \log \hat{Z}}{\partial w_k} w_k + \log \hat{Z} - c_k) \mathbf{h}_k$ and apply a second-order Taylor expansion to $\log \hat{Z}$. The resulting expression $\mathbf{g} = \sum_k (f_k + f_{-k} - c_k) \mathbf{h}_k$ separates terms f_k that contribute to the expected gradient from terms f_{-k} that have zero expectation and thus only contribute to the variance (cf. Appendix B):

$$f_k \approx \frac{w_k^2}{2K^2 Z^2} \quad (6)$$

$$f_{-k} \approx \log Z - \frac{3}{2} + \frac{2}{KZ} \sum_{l \neq k} w_l - \frac{1}{2K^2 Z^2} \left(\sum_{l \neq k} w_l \right)^2. \quad (7)$$

Since f_{-k} and c_k are independent of \mathbf{h}_k , the expected gradient is (cf. Appendix C.1):

$$\mathbb{E}[\mathbf{g}] = \sum_k \mathbb{E}[f_k \mathbf{h}_k] \approx \frac{1}{2Z^2 K} \mathbb{E}_1 [w_1^2 \mathbf{h}_1] = \mathcal{O}(K^{-1}), \quad (8)$$

where \mathbb{E}_1 denotes an expectation over the first latent distribution $q_\phi(\mathbf{z}_1|\mathbf{x})$. Since the choice of control variates $c_k = c_k(\mathbf{z}_{-k})$ is free, we can choose $c_k = f_{-k}$ to cancel out all zero expectation terms. The resulting covariance, derived in Appendix C.2, is:

$$\text{Cov}[\mathbf{g}] = \text{Cov} \left[\sum_k f_k \mathbf{h}_k \right] \approx \frac{1}{4K^3 Z^4} \text{Cov}_1 [w_1^2 \mathbf{h}_1] = \mathcal{O}(K^{-3}) \quad (9)$$

with Cov_1 indicating the covariance over $q_\phi(\mathbf{z}_1|\mathbf{x})$. Although as we discuss in Section 4 this is not the minimal variance choice of control variates, it is sufficient to achieve an SNR of $\mathcal{O}(K^{1/2})$.

4 Optimal Control Variate

The analysis above shows that in theory it is possible to attain a good SNR with the score function estimator. In this section we derive the optimal (in terms of variance of the resulting estimator) control variates $\{c_k\}_{k=1}^K$ by decomposing $\mathbf{g} = \sum_k (f_k + f_{-k} - c_k) \mathbf{h}_k$ as above, and minimizing the trace of the covariance matrix, i.e. $\mathbb{E}[\|\mathbf{g}\|^2] - \|\mathbb{E}[\mathbf{g}]\|^2$. Since $\mathbb{E}[f_{-k} \mathbf{h}_k]$ and $\mathbb{E}[c_k \mathbf{h}_k]$ are both zero, $\mathbb{E}[\mathbf{g}] = \nabla_\phi \mathcal{L}_K$ does not depend on c_k . Thus, the minimization only involves the first term:

$$\begin{aligned} \frac{1}{2} \frac{\partial}{\partial c_k} \mathbb{E}[\|\mathbf{g}\|^2] &= \mathbb{E} \left[\mathbf{h}_k^T \sum_l (f_l + f_{-l} - c_l) \mathbf{h}_l \right] \\ &= \mathbb{E}_{-k} \left[\sum_l \mathbb{E}_k [f_l \mathbf{h}_k^T \mathbf{h}_l] + (f_{-k} - c_k) \mathbb{E}_k [\|\mathbf{h}_k\|^2] \right]. \end{aligned}$$

where \mathbb{E}_k and \mathbb{E}_{-k} indicate expectations over $q_\phi(\mathbf{z}_k|\mathbf{x})$ and $q_\phi(\mathbf{z}_{-k}|\mathbf{x})$, respectively. Setting the argument of \mathbb{E}_{-k} to zero, we get the optimal control variates $c_k = c_k(\mathbf{z}_{-k})$ and gradient estimator \mathbf{g} :

$$c_k = f_{-k} + \sum_l \frac{\mathbb{E}_k [f_l \mathbf{h}_k^T \mathbf{h}_l]}{\mathbb{E}_k [\|\mathbf{h}_k\|^2]} \quad (10)$$

$$\mathbf{g} = \sum_k \left(f_k - \sum_l \frac{\mathbb{E}_k [f_l \mathbf{h}_k^T \mathbf{h}_l]}{\mathbb{E}_k [\|\mathbf{h}_k\|^2]} \right) \mathbf{h}_k. \quad (11)$$

Applying (11) in practice requires marginalizing over one latent variable and decoupling terms that do not depend on \mathbf{z}_k from those that do. In the remainder of this section we will 1) make a series of approximations to keep computation tractable, and 2) consider two limiting cases for the *effective sample size* (ESS) [25] in which we can decouple terms.

Simplifying approximations to Equation (11) First, we consider a term with $l \neq k$, define $\Delta f_l := f_l - \mathbb{E}_k[f_l]$, and subtract and add $\mathbb{E}_k[f_l]$ from inside the expectation:

$$\mathbb{E}_k [f_l \mathbf{h}_k^T] \mathbf{h}_l = \mathbb{E}_k [\Delta f_l \mathbf{h}_k^T] \mathbf{h}_l + \mathbb{E}_k[f_l] \mathbb{E}_k [\mathbf{h}_k^T] \mathbf{h}_l = \mathbb{E}_k [\Delta f_l \mathbf{h}_k^T] \mathbf{h}_l$$

where we used the fact that $\mathbb{E}_k [\mathbf{h}_k] = 0$. The $l \neq k$ terms thus only contribute to fluctuations relative to a mean value, and we assume they can be neglected.

Second, we assume that $|\phi|$, the number of parameters of q_ϕ , is large, and the terms of the sum $\|\mathbf{h}_k\|^2 = \sum_{i=1}^{|\phi|} h_{ki}^2$ are approximately independent with finite variances σ_i^2 . By the Central Limit Theorem we approximate the distribution of $\Delta \|\mathbf{h}_k\|^2 := \|\mathbf{h}_k\|^2 - \mathbb{E}_k [\|\mathbf{h}_k\|^2]$ with a zero-mean Gaussian with standard deviation $(\sum_{i=1}^{|\phi|} \sigma_i^2)^{1/2}$. Seeing that $\mathbb{E}_k [\|\mathbf{h}_k\|^2]$ is $\mathcal{O}(|\phi|)$, we have

$$\frac{\mathbb{E}_k [f_k \|\mathbf{h}_k\|^2]}{\mathbb{E}_k [\|\mathbf{h}_k\|^2]} = \mathbb{E}_k [f_k] + \frac{\mathbb{E}_k [f_k \Delta \|\mathbf{h}_k\|^2]}{\mathbb{E}_k [\|\mathbf{h}_k\|^2]} = \mathbb{E}_k [f_k] + \mathcal{O}(|\phi|^{-1/2}),$$

where we used that the argument in the numerator scales as $(\sum_{i=1}^{|\phi|} \sigma_i^2)^{1/2} = \mathcal{O}(|\phi|^{1/2})$.

Finally, the expectation can be approximated with a sample average. Writing $f_k = f_k(\mathbf{z}_k, \mathbf{z}_{-k})$ and drawing S new samples $\mathbf{z}^{(1)}, \dots, \mathbf{z}^{(S)} \sim q_\phi(\mathbf{z}|\mathbf{x})$:

$$\mathbb{E}_k [f_k] \approx \frac{1}{S} \sum_{s=1}^S f_k(\mathbf{z}^{(s)}, \mathbf{z}_{-k}).$$

This will introduce additional fluctuations with scale $S^{-1/2}$. The S samples can be reused for all K terms and the $S + K$ samples can all be used to evaluate the gradients of the generative model.

Putting these three approximations together and using $d_k(\mathbf{z}_k, \mathbf{z}_{-k}) = f_k(\mathbf{z}_k, \mathbf{z}_{-k}) + f_{-k}(\mathbf{z}_{-k})$, we obtain the sample-based expression of the OVIS estimator, called OVIS_{MC} in the following:

$$\text{OVIS}_{\text{MC}} : \quad \mathbf{g} \approx \sum_k \left(d_k(\mathbf{z}_k, \mathbf{z}_{-k}) - \frac{1}{S} \sum_{s=1}^S d_k(\mathbf{z}^{(s)}, \mathbf{z}_{-k}) \right) \mathbf{h}_k. \quad (12)$$

Effective sample size (ESS) The ESS [25] is a commonly used yardstick of the efficiency of an importance sampling estimate, defined as

$$\text{ESS} := \frac{(\sum_k w_k)^2}{\sum_k w_k^2} = \frac{1}{\sum_k v_k^2} \in [1, K]. \quad (13)$$

A low ESS occurs when only a few weights dominate, which indicates that the proposal distribution q poorly matches p . In the opposite limit, the variance of importance weights is finite and the ESS will scale with K . Therefore the limit $\text{ESS} \gg 1$ corresponds to the asymptotic limit studied in Section 3.

Optimal control for ESS limits and unified interpolation We first consider $\text{ESS} \gg 1$ and for each k we introduce the unnormalized leave- w_k -out approximation to \hat{Z} :

$$\tilde{Z}_{[-k]} := \frac{1}{K} \sum_{l \neq k} w_l \quad \text{such that} \quad \hat{Z} - \tilde{Z}_{[-k]} = \frac{w_k}{K}. \quad (14)$$

Assuming $\text{Var}[w_k] < \infty$, this difference is $\mathcal{O}(K^{-1})$ as $K \rightarrow \infty$, thus we can expand $\log \hat{Z}$ around $\hat{Z} = \tilde{Z}_{[-k]}$. In this limit, the optimal control variate simplifies to the non-trivial (cf. Appendix D.1):

$$\text{ESS} \gg 1 : \quad c_k \approx \log \tilde{Z}_{[-k]} = \log \frac{1}{K} \sum_{l \neq k} w_l. \quad (15)$$

When $\text{ESS} \approx 1$, one weight is much larger than the others and the assumption above is no longer valid. To analyze this frequently occurring scenario, assume that $k' = \arg\max_l w_l$ and $w_k \gg \sum_{l \neq k'} w_l$. In this limit $\log \hat{Z} \approx \log w_{k'}/K$ and $v_k \approx \delta_{k,k'}$ and thus $d_k = \log w_{k'}/K - \delta_{k,k'}$. In Appendix D.2 we show we can approximate Equation (10) with

$$\text{ESS} \approx 1 : \quad c_k \approx \log \hat{Z}_{[-k]} - \delta_{k,k'} = \log \frac{1}{K-1} \sum_{l \neq k} w_l - \delta_{k,k'} . \quad (16)$$

We can now introduce OVIS_\sim , the gradient estimator that unifies the two ESS limits based on the approximation $v_k \approx \delta_{k,k'}$ (Appendix D.3), with the following control variate:

$$\text{OVIS}_\sim : \quad c_k^\gamma := \log \hat{Z}_{[-k]} - \gamma v_k + (1 - \gamma) \log \left(1 - \frac{1}{K} \right) \quad \gamma \in [0, 1] . \quad (17)$$

OVIS_\sim is unbiased for $\gamma = 0$. In this paper we will only conduct experiments for the two limiting cases $\gamma = 0$, corresponding to Equation (15), and $\gamma = 1$ approximating Equation (16).

Higher ESS with looser lower bound Empirically we observe that training may be impaired by a low ESS and by *posterior collapse* [4, 26–29]. This motivates trading the tight IWAE objective for a gradient estimator with higher ESS. To that end, we use the importance weighted Rényi (IWR) bound:

$$\mathcal{L}_K^\alpha(\mathbf{x}) := \frac{1}{1 - \alpha} \mathbb{E} [\log \hat{Z}(\alpha)] \quad \hat{Z}(\alpha) := \frac{1}{K} \sum_k w_k^{1-\alpha} \quad (18)$$

which for $\alpha \in [0, 1]$ is a lower bound on the Rényi objective $\log \mathbb{E}_1 [w_1^{1-\alpha}] / (1 - \alpha)$ [30]. The Rényi objective in itself coincides with $\log p(\mathbf{x})$ for $\alpha = 0$ and is monotonically non-increasing in α , i.e. is an evidence lower bound [30]. So we have a looser bound but higher $\text{ESS}(\alpha) = 1 / \sum_k v_k^2(\alpha) \geq \text{ESS}(0)$ for $\alpha \in [0, 1]$ with $v_k(\alpha) = w_k^{1-\alpha} / \sum_l w_l^{1-\alpha}$. In Appendix E we derive the score function estimator and control variate expressions for \mathcal{L}_K^α . The objective can either be used in a warm-up scheme by gradually decreasing $\alpha \rightarrow 0$ throughout iterations or can be run with a constant $0 < \alpha < 1$.

5 Related Work

The score function estimator with control variates can be used with all the commonly used variational families. By contrast, the reparameterization trick is only applicable under specific conditions. We now give a brief overview of the existing alternatives and refer the reader to [31] for a more extensive review. The importance of handling discrete distributions without relaxations is discussed in [9].

NVIL [13], DARN [17], and MuProp [18] demonstrate that score function estimators with carefully crafted control variates allow to train deep generative models. VIMCO [14] extends this to multi-sample objectives, and recycles the Monte Carlo samples \mathbf{z}_{-k} to define a control variate $c_k = c_k(\mathbf{z}_{-k})$. Unlike OVIS, VIMCO only controls the variance of the term $\log \hat{Z}$ in $d_k = \log \hat{Z} - v_k$, leaving v_k uncontrolled, and causing the SNR to decrease with the number of particles K as we empirically observe in Section 6.1. We provide a detailed review of VIMCO in Appendix F.

The Reweighted Wake-Sleep (RWS) algorithm [20] is an extension of the original Wake-Sleep algorithm (ws) [19] that alternates between two distinct learning phases for optimizing importance weighted objectives. A detailed review of RWS and ws is available in Appendix F.

The Thermodynamic Variational Objective (TVO) [21] is a lower bound to $\log p_\theta(\mathbf{x})$ that stems from a Riemannian approximation of the Thermodynamic Variational Identity (TVI), and unifies the objectives of Variational Inference and Wake-Sleep. Evaluating the gradient involves differentiating through an expectation over a distribution with an intractable normalizing constant. To accommodate this, the authors propose an estimator that generalizes the score function estimator based on a tractable covariance term. We review the TVO in more detail in Appendix F.

Given a deterministic *sampling path* $g(\epsilon; \theta)$ such that $\mathbf{z} \sim p_\theta(\mathbf{z})$ and $\mathbf{z} = g(\epsilon; \theta), \epsilon \sim p(\epsilon)$ are equivalent, one can derive a *pathwise gradient estimator* of the form $\nabla_\theta \mathbb{E}_{p_\theta(\mathbf{z})} [f_\theta(\mathbf{z})] = \mathbb{E}_{p(\epsilon)} [\nabla_\theta f_\theta(g(\epsilon; \theta))]$. This estimator – introduced in machine learning as the *reparameterization trick* or *stochastic backpropagation* [2, 3] – exhibits low variance thanks to the structural information

provided by the sampling path. Notably, a zero expectation term can be removed from the estimator [32]. Extending on this, [24] derives an alternative gradient estimator for IWAE that exhibits $\text{SNR} \sim K^{1/2}$, as opposed to $\text{SNR} \sim K^{-1/2}$ for the *standard* IWAE objective [23].

Continuous relaxations of discrete distributions yield a biased low-variance gradient estimate thanks to the reparameterization trick [16, 33]. Discrete samples can be obtained using the Straight-Through estimator [5, 34]. The resulting gradient estimate remains biased, but can be used as a control variate for the score function objective, resulting in an unbiased low-variance estimate of the gradient [15, 35].

6 Experimental Results

We conduct a number of experiments¹ on benchmarks that have previously been used to test score function based estimators. All models are trained via stochastic gradient ascent using the Adam optimizer [36] with default parameters. We use regular gradients on the training objective for the generative model parameters θ . The SNR for θ scales as $\mathcal{O}(K^{1/2})$ [23].

6.1 Asymptotic Variance

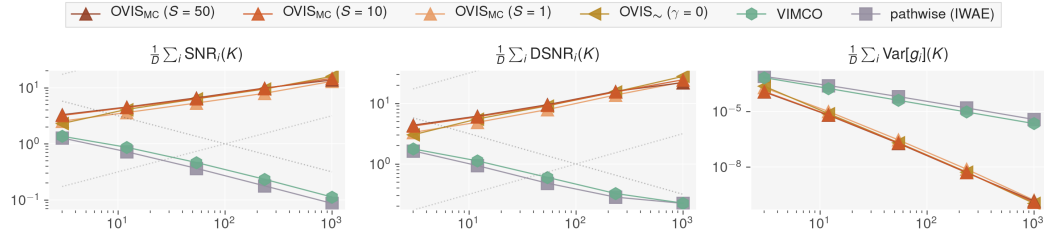


Figure 1: Gaussian model. Parameter-wise average of the asymptotic SNR, DSNR and variance of the gradients of the parameter b for different number of particles $K \in [3, 1000]$ using 10^4 MC samples. The dotted lines stand for $y = 10^{\pm 1} K^{\pm 0.5}$.

Following [23], we empirically corroborate the asymptotic properties of the OVIS gradient estimator by means of the following simple model:

$$\mathbf{z} \sim \mathcal{N}(\mathbf{z}; \boldsymbol{\mu}, \mathbf{I}), \quad \mathbf{x}|\mathbf{z} \sim \mathcal{N}(\mathbf{x}; \mathbf{z}, \mathbf{I}), \quad q_\phi(\mathbf{z}|\mathbf{x}) = \mathcal{N}(\mathbf{z}; \mathbf{A}\mathbf{x} + \mathbf{b}, \frac{2}{3}\mathbf{I}).$$

where \mathbf{x} and \mathbf{z} are real vectors of size $D = 20$. We sample $N = 1024$ points $\{\mathbf{x}^{(n)}\}_{n=1}^N$ from the *true* model where $\boldsymbol{\mu}^* \sim \mathcal{N}(\mathbf{0}, \mathbf{I})$. The optimal parameters are $\mathbf{A}^* = \mathbf{I}/2$, $\mathbf{b}^* = \boldsymbol{\mu}^*/2$, and $\boldsymbol{\mu}^* = \frac{1}{N} \sum_{n=1}^N \mathbf{x}^{(n)}$. The model parameters are obtained by adding Gaussian noise of scale $\epsilon = 10^{-3}$. We measure the variance and the SNR of the gradients with 10^4 MC samples. We also measured the *directional* SNR (DSNR [23]) to probe if our results hold in the multidimensional case.

In Figure 1 we report the gradient statistics for \mathbf{b} . We observe that using more samples in the standard IWAE leads to a decrease in SNR as $\mathcal{O}(K^{-1/2})$ for both VIMCO and the pathwise-IWAE [23]. The tighter variance control provided by OVIS leads the variance to decrease almost at a rate $\mathcal{O}(K^{-3})$, resulting in a measured SNR not far from $\mathcal{O}(K^{1/2})$ both for OVIS_{MC} and OVIS_\sim . This shows that, despite the approximations, the proposed gradient estimators OVIS_{MC} and OVIS_\sim are capable of achieving the theoretical SNR of $\mathcal{O}(K^{1/2})$ derived in the asymptotic analysis in Section 3.

In Appendix G, we learn the parameters of the Gaussian model using OVIS, RWS, VIMCO and the TVO. We find that optimal variance reduction translates into a more accurate estimation of the optimal parameters of the inference network when compared to RWS, VIMCO and the TVO.

6.2 Gaussian Mixture Model

We evaluate OVIS on a Gaussian Mixture Model and show that, unlike VIMCO [9], our method yields better inference networks as the number of particles K increases. Following [9], we define:

$$p_\theta(z) = \text{Cat}(z|\text{softmax}(\theta)) \quad p(x|z) = \mathcal{N}(x|\mu_z, \sigma_z^2) \quad q_\phi(z|x) = \text{Cat}(z|\text{softmax}(\eta_\phi(x)))$$

¹The full experimental framework is available at github.com/vlievin/ovis

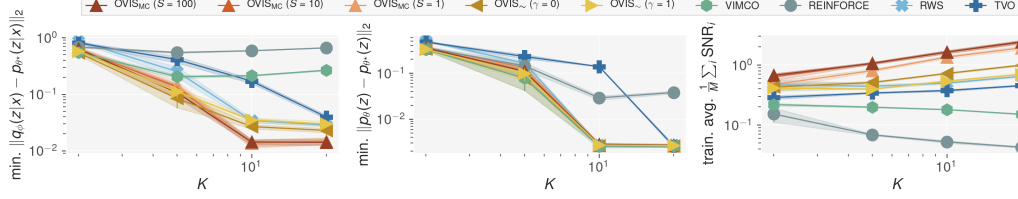


Figure 2: Training of the Gaussian mixture model. Minimum test-diagnostics recorded during training and training average of the SNR of the gradients of ϕ with $M = \text{card}(\phi)$. In contrast to VIMCO, OVIS_\sim and OVIS_{MC} all benefit from the increase of the particles budget, OVIS_{MC} yields the most accurate posterior among the compared methods.

where $z \in \{0, \dots, C-1\}$, $\mu_z = 10z$, $\sigma_z = 5$, and $C = 20$ is the number of clusters. The inference network η_ϕ is parameterized by a multilayer perceptron with architecture 1–16– C and tanh activations. The true generative model is set to $p_{\theta^*}(z = c) = (c + 5) / \sum_{i=1}^C (i + 5)$.

All models are trained for 100k steps with 5 random seeds. We compare OVIS with VIMCO, RWS, Reinforce, and the TVO. For the latter we chose to use 5 partitions and $\beta_1 = 10^{-2}$, after a hyperparameter search over $\beta_1 \in \{10^{-1}, 10^{-1.5}, 10^{-2}, 10^{-2.5}, 10^{-3}\}$ and $\{2, 5\}$ partitions.

Each model is evaluated on a held-out test set of size $M = 100$. We measure the accuracy of the learned posterior $q_\phi(z|x)$ by its average L_2 distance from the true posterior, i.e. $\frac{1}{M} \sum_{m=1}^M \|q_\phi(z|x^{(m)}) - p_{\theta^*}(z|x^{(m)})\|_2$. As a sanity check, we assess the quality of the generative model using $\|\text{softmax}(\theta) - \text{softmax}(\theta^*)\|_2$. The SNR of the gradients for the parameters ϕ is evaluated on one mini-batch of data using 500 MC samples.

We report our main results in Figure 2, and training curves (including ESS) in Appendix H. In contrast to VIMCO, the accuracy of the posteriors learned using OVIS_{MC} and OVIS_\sim all improve monotonically with K and outperform the baseline estimators, independently of the choice of the number of auxiliary particles S . All OVIS methods outperform the state-of-the-art estimators RWS and the TVO as measured by the L_2 distance between the approximate and the true posterior. Furthermore, even if exceeded by the sampled-based OVIS_{MC} , $\text{OVIS}_\sim(\gamma = 0)$ gives slightly more accurate solutions than its counterpart $\text{OVIS}_\sim(\gamma = 1)$, which is expected since $\text{ESS} = \mathcal{O}(K)$ is observed in this experiment.

6.3 Deep Generative Models

We utilize the OVIS estimators to learn the parameters of both discrete and continuous deep generative models using stochastic gradient ascent. The base learning rate is fixed to $3 \cdot 10^{-4}$, we use mini-batches of size 24 and train all models for $4 \cdot 10^6$ steps. We use the statically binarized MNIST dataset [37] with the original training/validation/test splits of size 50k/10k/10k. We follow the experimental protocol as detailed in [21], including the β partition for the TVO and the exact architecture of the models. We use a three-layer Sigmoid Belief Network [38] as an archetype of discrete generative model [13, 14, 21] and a Gaussian Variational Autoencoder [2] with 200 latent variables. All models are trained with 2 initial random seeds and for $K \in \{5, 10, 50\}$ particles.

We assess the performance based on the marginal log-likelihood estimate $\log \hat{p}_\theta(\mathbf{x}) = \mathcal{L}_{5000}(\mathbf{x})$, that we evaluate on 10k *training* data points, such as to disentangle the training dynamics from the regularisation effect that is specific to each method. We measure the quality of the inference network solution using the divergence $\mathcal{D}_{\text{KL}}(q_\phi(\mathbf{z}|\mathbf{x})||p_\theta(\mathbf{z}|\mathbf{x})) \approx \log \hat{p}_\theta(\mathbf{x}) - \mathcal{L}_1(\mathbf{x})$. The full training curves – including the test log likelihood and divergences – are available in Appendix I.

We learn the parameters of the SBN using the OVIS estimators for the IWAE bound and use VIMCO as a baseline. We report $\log \hat{p}_\theta(\mathbf{x})$ in the left plot of Figure 3. All OVIS methods outperform VIMCO, ergo supporting the advantage of optimal variance reduction. When using a small number of particles $K = 5$, learning can be greatly improved by using an accurate MC estimate of the optimal control variate, as suggested by $\text{OVIS}_{\text{MC}}(S = 50)$ which allows gaining +1.0 nats over VIMCO. While $\text{OVIS}(\gamma = 0)$, designed for large ESS slightly improved over VIMCO, the biased $\text{OVIS}_\sim(\gamma = 1)$ for low ESS performed significantly better than other methods for $K \geq 10$, which

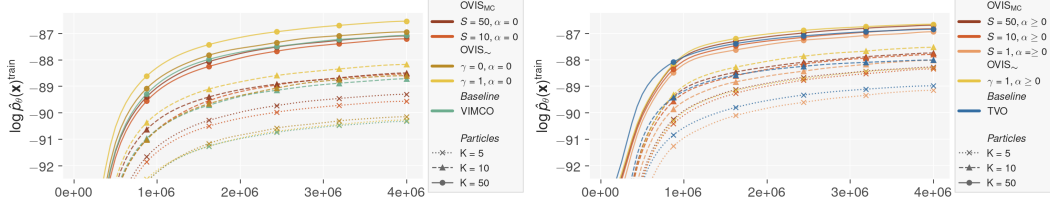


Figure 3: Training a Sigmoid Belief Network on Binarized MNIST. (Left) Optimizing for the importance weighted bound \mathcal{L}_K using OVIS. (Right) Optimizing for the Rényi importance lower bound \mathcal{L}_K^α using OVIS with α annealing $0.99 \rightarrow 0$. The curves are averaged over two seeds and smoothed for clarity.

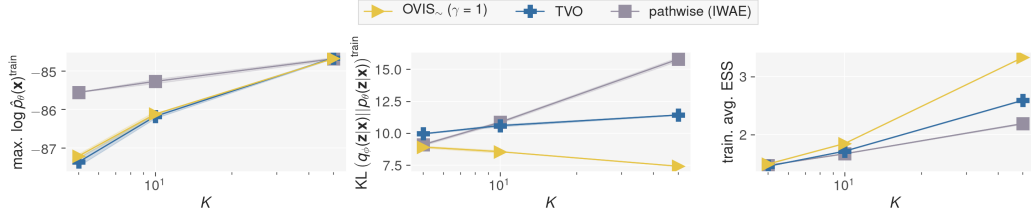


Figure 4: Training a one layer Gaussian VAE. Maximum recorded training $\log \hat{p}_\theta(\mathbf{x})$, final estimate of the bound $\mathcal{D}_{\text{KL}}(q_\phi(\mathbf{z}|\mathbf{x})||p_\theta(\mathbf{z}|\mathbf{x}))$ and training average of the ESS. OVIS yields similar likelihood performances as the TVO but benefits from a tighter bound thanks to optimizing for the IWR bound.

coincides with the ESS measured in the range $[1.0, 3.5]$ for all methods. We attribute the relative decrease of performances observed for OVIS_{MC} for $K = 50$ to *posterior collapse*.

In Figure 3 (right) we train the SBN using OVIS and the TVO. OVIS is coupled with the objective \mathcal{L}_K^α for which we anneal the parameter α from 0.99 to 0 during $1e6$ steps using geometric interpolation. For all K values, we have $\text{OVIS}_\sim(\gamma = 1) \geq \text{OVIS}_{\text{MC}}(S = 50) \geq \text{OVIS}_{\text{MC}}(S = 10) \geq \text{TVO} \geq \text{OVIS}_{\text{MC}}(S = 1)$.

In Figure 4 we train the IWAE with the pathwise estimator, the TVO and OVIS to learn the parameters of the VAE. OVIS is applied to the IWR bound with $\alpha = 0.7$. As measured by the training likelihood, OVIS methods perform on par with the TVO, which bridges the gap to the reparameterization trick for $K = 50$, although different objectives are at play. Measuring the quality of the learned proposals $q_\phi(\mathbf{z}|\mathbf{x})$ using the KL divergence allows disentangling the two methods, as $\text{OVIS}(\gamma = 1)$ applied to the IWVR bound outputs higher-quality posteriors for all considered number of particles, which in turn results in a higher ESS.

$\text{OVIS}_\sim(\gamma = 1)$ generates training dynamics that are superior to the baseline TVO and to the sample-based OVIS_{MC} for $K \geq 10$ – without incurring a supplementary cost of S auxiliary samples. We interpret this result as a consequence of the ESS-specific design, which also appeared to be robust to the choice of the class of IWR objectives. This also corroborates the results of [32], that suppressing the prefactor terms v_k benefits learning. Nevertheless, the good performance of $\text{OVIS}(\gamma = 0)$ in the experiments 6.1 and 6.2 supports the need for adapting the control variate based on the ESS.

7 Conclusion

We proposed OVIS, a gradient estimator that is generally applicable to deep models with stochastic variables, and is empirically shown to have optimal variance control. This property is achieved by identifying and canceling terms in the estimator that solely contribute to the variance. We expect that in practice it will often be a good trade-off to use a looser bound with a higher effective sample size, e.g. by utilizing the OVIS estimator with the importance weighted Rényi bound, allowing control of this trade-off via an additional scalar smoothing parameter. This sentiment is supported by our method demonstrating better performance than the current state-of-the-art.

References

- [1] David M Blei, Andrew Y Ng, and Michael I Jordan. Latent dirichlet allocation. *Journal of machine Learning research*, 3(Jan):993–1022, 2003.
- [2] Diederik P Kingma and Max Welling. Auto-encoding variational bayes. *arXiv preprint arXiv:1312.6114*, 2013.
- [3] Danilo Jimenez Rezende, Shakir Mohamed, and Daan Wierstra. Stochastic backpropagation and approximate inference in deep generative models. *arXiv preprint arXiv:1401.4082*, 2014.
- [4] Samuel R Bowman, Luke Vilnis, Oriol Vinyals, Andrew M Dai, Rafal Jozefowicz, and Samy Bengio. Generating sentences from a continuous space. *arXiv preprint arXiv:1511.06349*, 2015.
- [5] Aaron van den Oord, Oriol Vinyals, et al. Neural discrete representation learning. In *Advances in Neural Information Processing Systems*, pages 6306–6315, 2017.
- [6] Irina Higgins, Loic Matthey, Arka Pal, Christopher Burgess, Xavier Glorot, Matthew Botvinick, Shakir Mohamed, and Alexander Lerchner. beta-vae: Learning basic visual concepts with a constrained variational framework. *Iclr*, 2(5):6, 2017.
- [7] Lars Maaløe, Marco Fraccaro, Valentin Liévin, and Ole Winther. BIVA: A very deep hierarchy of latent variables for generative modeling. In *Advances in neural information processing systems*, pages 6548–6558, 2019.
- [8] Richard S Sutton, David A McAllester, Satinder P Singh, and Yishay Mansour. Policy gradient methods for reinforcement learning with function approximation. In *Advances in neural information processing systems*, pages 1057–1063, 2000.
- [9] Tuan Anh Le, Adam R Kosior, N Siddharth, Yee Whye Teh, and Frank Wood. Revisiting reweighted wake-sleep. *arXiv preprint arXiv:1805.10469*, 2018.
- [10] SM Ali Eslami, Nicolas Heess, Theophane Weber, Yuval Tassa, David Szepesvari, Geoffrey E Hinton, et al. Attend, infer, repeat: Fast scene understanding with generative models. In *Advances in Neural Information Processing Systems*, pages 3225–3233, 2016.
- [11] Yishu Miao and Phil Blunsom. Language as a latent variable: Discrete generative models for sentence compression. *arXiv preprint arXiv:1609.07317*, 2016.
- [12] Ronald J Williams. Simple statistical gradient-following algorithms for connectionist reinforcement learning. *Machine learning*, 8(3-4):229–256, 1992.
- [13] Andriy Mnih and Karol Gregor. Neural variational inference and learning in belief networks. *arXiv preprint arXiv:1402.0030*, 2014.
- [14] Andriy Mnih and Danilo J Rezende. Variational inference for monte carlo objectives. *arXiv preprint arXiv:1602.06725*, 2016.
- [15] George Tucker, Andriy Mnih, Chris J Maddison, John Lawson, and Jascha Sohl-Dickstein. Rebar: Low-variance, unbiased gradient estimates for discrete latent variable models. In *Advances in Neural Information Processing Systems*, pages 2627–2636, 2017.
- [16] Chris J Maddison, Andriy Mnih, and Yee Whye Teh. The concrete distribution: A continuous relaxation of discrete random variables. *arXiv preprint arXiv:1611.00712*, 2016.
- [17] Karol Gregor, Ivo Danihelka, Andriy Mnih, Charles Blundell, and Daan Wierstra. Deep autoregressive networks. *arXiv preprint arXiv:1310.8499*, 2013.
- [18] Shixiang Gu, Sergey Levine, Ilya Sutskever, and Andriy Mnih. Muprop: Unbiased backpropagation for stochastic neural networks. *arXiv preprint arXiv:1511.05176*, 2015.
- [19] Geoffrey E Hinton, Peter Dayan, Brendan J Frey, and Radford M Neal. The "wake-sleep" algorithm for unsupervised neural networks. *Science*, 268(5214):1158–1161, 1995.

- [20] Jörg Bornschein and Yoshua Bengio. Reweighted wake-sleep. *arXiv preprint arXiv:1406.2751*, 2014.
- [21] Vaden Masrani, Tuan Anh Le, and Frank Wood. The thermodynamic variational objective. In *Advances in Neural Information Processing Systems*, pages 11521–11530, 2019.
- [22] Yuri Burda, Roger Grosse, and Ruslan Salakhutdinov. Importance weighted autoencoders. *arXiv preprint arXiv:1509.00519*, 2015.
- [23] Tom Rainforth, Adam R Kosiorek, Tuan Anh Le, Chris J Maddison, Maximilian Igl, Frank Wood, and Yee Whye Teh. Tighter variational bounds are not necessarily better. *arXiv preprint arXiv:1802.04537*, 2018.
- [24] George Tucker, Dieterich Lawson, Shixiang Gu, and Chris J Maddison. Doubly reparameterized gradient estimators for monte carlo objectives. *arXiv preprint arXiv:1810.04152*, 2018.
- [25] Augustine Kong. A note on importance sampling using standardized weights. *University of Chicago, Dept. of Statistics, Tech. Rep.*, 348, 1992.
- [26] Xi Chen, Diederik P Kingma, Tim Salimans, Yan Duan, Prafulla Dhariwal, John Schulman, Ilya Sutskever, and Pieter Abbeel. Variational lossy autoencoder. *arXiv preprint arXiv:1611.02731*, 2016.
- [27] Casper Kaae Sønderby, Tapani Raiko, Lars Maaløe, Søren Kaae Sønderby, and Ole Winther. Ladder variational autoencoders. In *Advances in neural information processing systems*, pages 3738–3746, 2016.
- [28] Durk P Kingma, Tim Salimans, Rafal Jozefowicz, Xi Chen, Ilya Sutskever, and Max Welling. Improved variational inference with inverse autoregressive flow. In *Advances in neural information processing systems*, pages 4743–4751, 2016.
- [29] Adji B Dieng, Yoon Kim, Alexander M Rush, and David M Blei. Avoiding latent variable collapse with generative skip models. *arXiv preprint arXiv:1807.04863*, 2018.
- [30] Yingzhen Li and Richard E Turner. Rényi divergence variational inference. In *Advances in Neural Information Processing Systems*, pages 1073–1081, 2016.
- [31] Shakir Mohamed, Mihaela Rosca, Michael Figurnov, and Andriy Mnih. Monte carlo gradient estimation in machine learning. *arXiv preprint arXiv:1906.10652*, 2019.
- [32] Geoffrey Roeder, Yuhuai Wu, and David K Duvenaud. Sticking the landing: Simple, lower-variance gradient estimators for variational inference. In *Advances in Neural Information Processing Systems*, pages 6925–6934, 2017.
- [33] Eric Jang, Shixiang Gu, and Ben Poole. Categorical reparameterization with gumbel-softmax. *arXiv preprint arXiv:1611.01144*, 2016.
- [34] Yoshua Bengio, Nicholas Léonard, and Aaron Courville. Estimating or propagating gradients through stochastic neurons for conditional computation. *arXiv preprint arXiv:1308.3432*, 2013.
- [35] Will Grathwohl, Dami Choi, Yuhuai Wu, Geoffrey Roeder, and David Duvenaud. Backpropagation through the void: Optimizing control variates for black-box gradient estimation. *arXiv preprint arXiv:1711.00123*, 2017.
- [36] Diederik P Kingma and Jimmy Ba. Adam: A method for stochastic optimization. *arXiv preprint arXiv:1412.6980*, 2014.
- [37] Ruslan Salakhutdinov and Iain Murray. On the quantitative analysis of deep belief networks. In *Proceedings of the 25th international conference on Machine learning*, pages 872–879, 2008.
- [38] Radford M Neal. Connectionist learning of belief networks. *Artificial intelligence*, 56(1): 71–113, 1992.

A Derivation of the Score Function Estimator

Given K samples, the objective being maximized is

$$\mathcal{L}_K(\mathbf{x}) := \mathbb{E} \left[\log \hat{Z} \right] \quad \hat{Z} := \frac{1}{K} \sum_{k=1}^K w_k \quad w_k := \frac{p_\theta(\mathbf{x}, \mathbf{z}_k)}{q_\phi(\mathbf{z}_k | \mathbf{x})}. \quad (19)$$

The gradients of the multi-sample objective \mathcal{L}_K with respect to the parameter ϕ can be expressed as a sum of two terms, one arising from the expectation $\mathbb{E}[\cdot]$ and one from $\log \hat{Z}$:

$$\nabla_\phi \mathcal{L}_K = \underbrace{\mathbb{E} \left[\log \hat{Z} \frac{\nabla_\phi q_\phi(\mathbf{z}_{1:K} | \mathbf{x})}{q_\phi(\mathbf{z}_{1:K} | \mathbf{x})} \right]}_{\text{(a)}} + \underbrace{\mathbb{E} \left[\nabla_\phi \log \hat{Z} \right]}_{\text{(b)}}.$$

The term **(a)** yields the traditional score function estimator

$$\begin{aligned} \text{(a)} &= \mathbb{E} \left[\log \hat{Z} \nabla_\phi \log q_\phi(\mathbf{z}_{1:K} | \mathbf{x}) \right] \\ &= \mathbb{E} \left[\log \hat{Z} \sum_{k=1}^K \nabla_\phi \log q_\phi(\mathbf{z}_k | \mathbf{x}) \right]. \end{aligned} \quad (20)$$

The term **(b)** is

$$\begin{aligned} \text{(b)} &= \mathbb{E} \left[\nabla_\phi \log \frac{1}{K} \sum_{k=1}^K w_k \right] \\ &= \mathbb{E} \left[\frac{1}{\frac{1}{K} \sum_{k=1}^K w_k} \nabla_\phi \frac{1}{K} \sum_{k=1}^K w_k \right] \\ &= \mathbb{E} \left[\frac{1}{\sum_{l=1}^K w_l} \sum_{k=1}^K \nabla_\phi w_k \right] \\ &= \mathbb{E} \left[\frac{1}{\sum_{l=1}^K w_l} \sum_{k=1}^K w_k \nabla_\phi \log w_k \right] \\ &= \mathbb{E} \left[\sum_{k=1}^K v_k \nabla_\phi \log w_k \right], \quad v_k = \frac{w_k}{\sum_{l=1}^K w_l} \\ &= -\mathbb{E} \left[\sum_{k=1}^K v_k \nabla_\phi \log q_\phi(\mathbf{z}_k | \mathbf{x}) \right]. \end{aligned} \quad (21)$$

The derivation yields a factorized expression of the gradients

$$\nabla_\phi \mathcal{L}_K = \mathbb{E}_{q_\phi(\mathbf{z}_{1:K} | \mathbf{x})} \left[\sum_{k=1}^K \left(\log \hat{Z} - v_k \right) \mathbf{h}_k \right] \quad \text{with} \quad \mathbf{h}_k := \nabla_\phi \log q_\phi(\mathbf{z}_k | \mathbf{x}). \quad (22)$$

B Asymptotic Analysis

We present here a short derivation and direct the reader to [23] for the fine prints of the proof. The main requirement is that w_k is bounded, so that $\hat{Z} - Z$ (with $Z = p(\mathbf{x})$) will converge to 0 almost surely as $K \rightarrow \infty$. We can also state this through the central limit theorem by noting that $\hat{Z} - Z = \frac{1}{K} \sum_k (w_k - Z)$ is the sum of K independent terms so if $\text{Var}_1[w_1]$ is finite then $\hat{Z} - Z$ will converge to a Gaussian distribution with mean $\mathbb{E}[\hat{Z} - Z] = 0$ and variance $\text{Var}[\hat{Z} - Z] = \frac{1}{K} \text{Var}_1[w_1]$. The K^{-1} factor on the variance follows from independence. This means that in a Taylor expansion in $\hat{Z} - Z$ higher order terms will be suppressed.

Rewriting \mathbf{g} in terms of $\log \hat{Z}$:

$$\mathbf{g} = \sum_k (d_k - c_k) \mathbf{h}_k = \sum_k \left(\log \hat{Z} - w_k \frac{\partial}{\partial w_k} \log \hat{Z} - c_k \right) \mathbf{h}_k \quad (23)$$

and using the second-order Taylor expansion of $\log \hat{Z}$ about Z :

$$\log \hat{Z} \approx \log Z + \frac{\hat{Z} - Z}{Z} - \frac{(\hat{Z} - Z)^2}{2Z^2} \quad (24)$$

we have

$$\log \hat{Z} \approx \log Z - \frac{3}{2} + \frac{2}{KZ} \sum_l w_l - \frac{1}{2K^2Z^2} \left(\sum_l w_l \right)^2 \quad (25)$$

$$\frac{\partial}{\partial w_k} \log \hat{Z} \approx \frac{2}{KZ} - \frac{1}{K^2Z^2} \sum_l w_l. \quad (26)$$

The term d_k can thus be approximated as follows:

$$\begin{aligned} d_k &= \log \hat{Z} - w_k \frac{\partial}{\partial w_k} \log \hat{Z} \\ &\approx \log Z - \frac{3}{2} + \frac{2}{KZ} \sum_{l \neq k} w_l - \frac{1}{2K^2Z^2} \left(\sum_l w_l \right)^2 + \frac{1}{K^2Z^2} w_k \sum_l w_l \\ &= \log Z - \frac{3}{2} + \frac{2}{KZ} \sum_{l \neq k} w_l - \frac{1}{2K^2Z^2} \left(\sum_{l \neq k} w_l \right)^2 + \frac{1}{2K^2Z^2} w_k^2 \end{aligned} \quad (27)$$

where we used

$$\left(\sum_l w_l \right)^2 = \left(\sum_{l \neq k} w_l \right)^2 + w_k^2 + 2w_k \sum_{l \neq k} w_l.$$

By separately collecting the terms that depend and do not depend on \mathbf{z}_k into $f_k = f_k(\mathbf{z}_k, \mathbf{z}_{-k})$ and $f_{-k} = f_{-k}(\mathbf{z}_{-k})$, respectively, we can rewrite the estimator \mathbf{g} as:

$$\mathbf{g} = \sum_k (f_k + f_{-k} - c_k) \mathbf{h}_k \quad (28)$$

and from (27) we have

$$f_k \approx \frac{w_k^2}{2K^2Z^2} \quad (29)$$

$$f_{-k} \approx \log Z - \frac{3}{2} + \frac{2}{KZ} \sum_{l \neq k} w_l - \frac{1}{2K^2Z^2} \left(\sum_{l \neq k} w_l \right)^2. \quad (30)$$

C Asymptotic Expectation and Variance

We derive here the asymptotic expectation and variance of the gradient estimator \mathbf{g} in the limit $K \rightarrow \infty$.

C.1 Expectation

If both f_{-k} and c_k are independent of \mathbf{z}_k , we can write:

$$\mathbb{E}[\mathbf{g}] = \mathbb{E} \left[\sum_k (f_k + f_{-k} - c_k) \mathbf{h}_k \right] = \sum_k \mathbb{E} [f_k \mathbf{h}_k] \quad (31)$$

where we used that $\mathbb{E}[f_{-k}\mathbf{h}_k]$ and $\mathbb{E}[c_k\mathbf{h}_k]$ are zero. In the limit $K \rightarrow \infty$, each term of the sum can be expanded with the approximation (29) and simplified:

$$\mathbb{E}[f_k\mathbf{h}_k] \approx \mathbb{E}\left[\frac{w_k^2}{2K^2Z^2}\mathbf{h}_k\right] = \frac{1}{2K^2Z^2}\mathbb{E}_1[w_1^2\mathbf{h}_1] \quad (32)$$

where \mathbb{E}_1 denotes an expectation over the posterior $q_\phi(\mathbf{z}_1|\mathbf{x})$. The last step follows from the fact that the latent variables $\{\mathbf{z}_k\}_{k=1}^K$ are i.i.d. and the argument of the expectation only depends on one of them. In conclusion, the expectation is:

$$\mathbb{E}[\mathbf{g}] = \sum_k \mathbb{E}[f_k\mathbf{h}_k] \approx \frac{1}{2K^2Z^2}\mathbb{E}_1[w_1^2\mathbf{h}_1] = \mathcal{O}(K^{-1}) \quad (33)$$

irrespective of f_{-k} and c_k .

C.2 Variance

If c_k is chosen to be $c_k(\mathbf{z}_{-k}) = f_{-k}(\mathbf{z}_{-k})$ then we can again use the approximation (29) for $K \rightarrow \infty$ and get the asymptotic variance:

$$\text{Var}[\mathbf{g}] = \text{Var}\left[\sum_k f_k\mathbf{h}_k\right] \quad (34)$$

$$\approx \text{Var}\left[\sum_k \frac{w_k^2}{2K^2Z^2}\mathbf{h}_k\right] \quad (35)$$

$$= \frac{1}{4K^4Z^4} \sum_k \text{Var}_k[w_k^2\mathbf{h}_k] \quad (36)$$

$$= \frac{1}{4K^3Z^4} \text{Var}_1[w_1^2\mathbf{h}_1] \quad (37)$$

$$= \mathcal{O}(K^{-3}) \quad (38)$$

where Var_k denotes the variance over the k th approximate posterior $q_\phi(\mathbf{z}_k|\mathbf{x})$, and we used the fact that the latent variables $\{\mathbf{z}_k\}_{k=1}^K$ are i.i.d. and therefore there are no covariance terms.

D Optimal Control for the ESS Limits and Unified Interpolation

D.1 Control Variate for Large ESS

In the gradient estimator $\mathbf{g} = \sum_k \left(\log \hat{Z} - \frac{\partial \log \hat{Z}}{\partial w_k} w_k - c_k\right) \mathbf{h}_k$, we consider the k th term in the sum, where we have that $\hat{Z} - \tilde{Z}_{[-k]} = \frac{w_k}{K} \rightarrow 0$ as $K \rightarrow \infty$. We can therefore expand $\log \hat{Z}$ as a Taylor series around $\hat{Z} = \tilde{Z}_{[-k]}$, obtaining:

$$\log \hat{Z} = \log \tilde{Z}_{[-k]} + \sum_{p=1}^{\infty} \frac{(-1)^{p+1}}{p} \left(\frac{w_k}{K\tilde{Z}_{[-k]}}\right)^p \quad (39)$$

$$\frac{\partial \log \hat{Z}}{\partial w_k} = \frac{1}{w_k} \sum_{p=1}^{\infty} (-1)^{p+1} \left(\frac{w_k}{K\tilde{Z}_{[-k]}}\right)^p. \quad (40)$$

Inserting these results into the gradient estimator and using the expression $\mathbf{g} = \sum_k (f_k + f_{-k} - c_k) \mathbf{h}_k$ we see that

$$f_{-k} = \log \tilde{Z}_{[-k]} \quad (41)$$

$$f_k = \sum_{p=1}^{\infty} (-1)^{p+1} \left(\frac{1}{p} - 1\right) \left(\frac{w_k}{K\tilde{Z}_{[-k]}}\right)^p \quad (42)$$

$$= \sum_{p=2}^{\infty} (-1)^p \left(1 - \frac{1}{p}\right) \left(\frac{w_k}{K\tilde{Z}_{[-k]}}\right)^p. \quad (43)$$

We now use this to simplify the optimal control variate (10) to leading order. Since f_k is order K^{-2} , the term $\mathbb{E}_k [f_k \|\mathbf{h}_k\|^2]$ will be of order K^{-2} as well. The $l \neq k$ terms $\mathbb{E}_k [f_l \mathbf{h}_k^T \mathbf{h}_l]$ get non-zero contributions only through the w_k term in f_l . As w_k appears in $\tilde{Z}_{[-l]}$ with a prefactor K^{-1} , we have $\mathbb{E}_k [f_l \mathbf{h}_k^T \mathbf{h}_l] = \mathcal{O}(K^{-3})$ for $l \neq k$, and the sum of these terms is $\mathcal{O}(K^{-2})$. Overall, this means that the second term in the control variate only gives a contribution of $\mathcal{O}(K^{-2})$ and thus can be ignored:

$$c_k \approx \log \tilde{Z}_{[-k]} = \log \frac{1}{K} \sum_{l \neq k} w_l. \quad (44)$$

Note that in the simplifying approximation in Section 4 we argue that the $l \neq k$ terms $\mathbb{E}_k [f_l \mathbf{h}_k^T \mathbf{h}_l]$ can be omitted and only the $l = k$ term retained. Here we show that their overall contribution is the same order as the $l = k$ term. These results are not in contradiction because here we are only discussing orders and not the size of terms.

D.2 Control Variate for Small ESS

In the case $\text{ESS} \approx 1$ we can write $\log \hat{Z}$ as a sum of two terms:

$$\log \hat{Z} = \log \frac{w_{k'}}{K} + \log \left(1 + \frac{K \tilde{Z}_{[-k']}}{w_{k'}} \right), \quad (45)$$

where $w_{k'}$ is the dominating weight. The first term dominates and the second can be ignored to leading order. We will leave out a derivation for non-leading terms for brevity. So the gradient estimator $\mathbf{g} = \sum_k \left(\log \hat{Z} - \frac{\partial \log \hat{Z}}{\partial w_k} w_k - c_k \right) \mathbf{h}_k$ simply becomes $\mathbf{g} \approx \sum_k \left(\log \frac{w_{k'}}{K} - \delta_{k,k'} - c_k \right) \mathbf{h}_k$. This corresponds to $f_k = \delta_{k,k'} \log w_{k'}$ and $f_{-k} = (1 - \delta_{k,k'}) \log w_{k'} - \delta_{k,k'} - \log K$. Inserting this into Equation (11) we get:

$$\mathbf{g} = \sum_k \left(f_k - \sum_l \frac{\mathbb{E}_k [f_l \mathbf{h}_k^T \mathbf{h}_l]}{\mathbb{E}_k [\|\mathbf{h}_k\|^2]} \right) \mathbf{h}_k = \left(\log w_{k'} - \frac{\mathbb{E}_{k'} [\log w_{k'} \|\mathbf{h}_{k'}\|^2]}{\mathbb{E}_{k'} [\|\mathbf{h}_{k'}\|^2]} \right) \mathbf{h}_{k'}. \quad (46)$$

D.3 Approximation to the Small-ESS Limit and Unified Objective

Estimating the expectation $\mathbb{E}_{k'}[\dots]$ in Equation (46) using i.i.d. samples from $q_\phi(\mathbf{z}|\mathbf{x})$ is computationally involved. Therefore we resort to the approximation $\mathbf{g} \approx \sum_k \left(\log \frac{w_{k'}}{K} - \delta_{k,k'} - c_k \right) \mathbf{h}_k$ and choose to approximate the control variate as

$$c_k \approx \log \hat{Z}_{[-k]} - v_k = \log \frac{1}{K-1} \sum_{l \neq k} w_l - v_k. \quad (47)$$

Relying on the approximation $\delta_{k,k'} \approx v_k$ corresponds to suppressing the term $-v_k$ of the prefactors $d_k = \log \hat{Z} - v_k$ and does not guarantee the resulting objective to be unbiased. Suppressing this term has been explored in depth for the pathwise gradient estimator [32]. The gradient estimator $\sum_k v_k \mathbf{h}_k$ corresponds to *wake-phase* update in RWS.

This approximation allows us to define the OVIS_\sim gradient estimator for a scalar $\gamma \in [0, 1]$:

$$c_k^\gamma := \log \hat{Z}_{[-k]} - \gamma \cdot v_k + (1 - \gamma) \cdot \log(1 - 1/K) \quad (48)$$

where

$$c_k^0 = \log \frac{1}{K-1} \sum_{l \neq k} w_l + \log \frac{K-1}{K} \quad (49)$$

$$c_k^1 = \log \frac{1}{K-1} \sum_{l \neq k} w_l - v_k. \quad (50)$$

E Rényi Importance Weighted Bound

All the analysis applied to the score function estimator for the importance weighted bound including asymptotic SNR can directly be carried over to the Rényi importance weighted bound $\mathcal{L}_K^\alpha(\mathbf{x})$ because all the independence properties are unchanged. The score function estimator of the gradient of ϕ is given by

$$\nabla_\phi \mathcal{L}_K^\alpha(\mathbf{x}) = \sum_k \left(\frac{1}{1-\alpha} \log \hat{Z}(\alpha) - v_k(\alpha) \right) \mathbf{h}_k, \quad v_k(\alpha) = \frac{w_k^{1-\alpha}}{\sum_l w_l^{1-\alpha}}. \quad (51)$$

The OVIS_{MC} formulation holds using $d_k = \frac{1}{1-\alpha} \log \hat{Z}(\alpha) - v_k(\alpha)$ within the equation 12. Similarly for the asymptotic expression OVIS_~, the unified control variate 17 becomes:

$$c_k^\gamma := \log \frac{1}{1-\alpha} \log \hat{Z}_{[-k]}(\alpha) - \gamma \cdot v_k + (1-\gamma) \cdot \log(1-1/K) \quad (52)$$

F Gradient Estimators Review

In this paper, gradient *ascent* is considered (i.e. maximizing the objective function). The expression of the gradient estimators presented below are therefore adapted for this setting.

VIMCO The formulation of the VIMCO [14] control variate exploits the structure of $\hat{Z} := \frac{1}{K} \sum_l w_l$ using $c_k := c_k(\mathbf{z}_{-k}) = \log \frac{1}{K} \sum_{l \neq k} w_l + \hat{w}_{[-k]}$ where $\hat{w}_{[-k]}$ stands for the arithmetic or geometric average of the weights w_l given the set of outer samples \mathbf{z}_{-k} . Defining $\log \hat{Z}_{[-k]} := c_k$, the VIMCO estimator of the gradients is

$$\nabla_\phi \mathcal{L}_K = \mathbb{E}_{q_\phi(\mathbf{z}_{1:K}|\mathbf{x})} \left[\underbrace{\sum_{k=1}^K \left(\log \hat{Z} - \log \hat{Z}_{[-k]} \right) \mathbf{h}_k}_{(\mathbf{a})} + \underbrace{\sum_{k=1}^K v_k \nabla_\phi \log w_k}_{(\mathbf{b})} \right]. \quad (53)$$

We refer to [14] for the derivation. Here, the term $\hat{Z}_{[-k]}$ can be expressed using the arithmetic and the geometric averaging [14]. The leave-one-sample estimate can be expressed as

$$\hat{Z}_{[-k]} = \frac{1}{K} \sum_{l \neq k} w_l + \hat{w}_{[-k]} \text{ with } \begin{cases} \hat{w}_{[-k]} = \frac{1}{K-1} \sum_{l \neq k} w_l & (\text{arithmetic}) \\ \hat{w}_{[-k]} = \exp \frac{1}{K-1} \sum_{l \neq k} \log w_l & (\text{geometric}) \end{cases} \quad (54)$$

The term **(b)** is well-behaved because it is a convex combination of the K gradients $\nabla_\phi \log w_k$. However, the term **(a)** may dominate the term **(b)**. In contrast to VIMCO, OVIS allows controlling the variance of both terms **(a)** and **(b)**, resulting in a more optimal variance reduction. In the Reweighted Wake Sleep (RWS) with wake-wake- ϕ update, the gradient of the parameters ϕ of the inference network corresponds to the negative of the term **(b)**.

Wake-sleep The algorithm [19] relies on two separate learning steps that are alternated during training: the *wake-phase* that updates the parameters of the generative model θ and the *sleep-phase* used to update the parameters of the inference network with parameters ϕ . During the *wake-phase*, the generative model is optimized to maximize the evidence lower bound \mathcal{L}_1 given a set of observation $\mathbf{x} \sim p(\mathbf{x})$. During the *sleep-phase*, a set of observations and latent samples are *dreamed* from the model: $\mathbf{x}, \mathbf{z} \sim p_\theta(\mathbf{x}, \mathbf{z})$ and the parameters ϕ of the inference network are optimized to minimize the KL divergence between the true posterior of the generative model and the approximate posterior: $\mathcal{D}_{\text{KL}}(p_\theta(\mathbf{z}|\mathbf{x})||q_\phi(\mathbf{z}|\mathbf{x}))$.

Reweighted Wake-Sleep (RWS) extends the original Wake-Sleep algorithm for importance weighted objectives [20]. The generative model is now optimized for the importance weighted bound \mathcal{L}_K , which gives the following gradients

$$\nabla_\theta \mathcal{L}_K = \mathbb{E}_{q_\phi(\mathbf{z}_{1:K}|\mathbf{x})} \left[\sum_k v_k \nabla_\theta \log w_k \right] \quad (\text{wake-phase } \theta). \quad (55)$$

The parameters ϕ of the inference network are optimized given two updates: the *sleep-phase* ϕ and the *wake-phase* ϕ . The *sleep-phase* ϕ is identical to the original Wake-Sleep algorithm, the gradients of the parameters ϕ of the inference model are given by

$$-\nabla_{\phi} \mathbb{E}_{p_{\theta}(\mathbf{x})} [\mathcal{D}_{\text{KL}}(p_{\theta}(\mathbf{z}_{1:K}|\mathbf{x})||q_{\phi}(\mathbf{z}_{1:K}|\mathbf{x}))] = \mathbb{E}_{p_{\theta}(\mathbf{z}_{1:K}, \mathbf{x})} \left[\sum_k \mathbf{h}_k \right] \quad (\text{sleep-phase } \phi). \quad (56)$$

The *wake-phase* ϕ differs from the original Wake-Sleep algorithm that samples \mathbf{x}, \mathbf{z} are sampled respectively from the dataset and from the inference model $q_{\phi}(\mathbf{z}|\mathbf{x})$. In this cases the gradients are given by:

$$-\nabla_{\phi} \mathbb{E}_{p(\mathbf{x})} [\mathcal{D}_{\text{KL}}(p_{\theta}(\mathbf{z}_{1:K}|\mathbf{x})||q_{\phi}(\mathbf{z}_{1:K}|\mathbf{x}))] = \mathbb{E}_{p(\mathbf{x})} \left[\mathbb{E}_{q_{\phi}(\mathbf{z}_{1:K}|\mathbf{x})} \left[\sum_k v_k \mathbf{h}_k \right] \right] \quad (\text{wake-phase } \phi). \quad (57)$$

Critically, in Variational Autoencoders one optimizes a lower bound of the marginal log-likelihood (\mathcal{L}_K), while RWS instead optimizes a biased estimate of the marginal log-likelihood $\log p(\mathbf{x})$. However, the bias decreases with K [20]. [9] shows that RWS is a method of choice for training deep generative models and stochastic control flows. In particular, [9] shows that increasing the budget of particles K benefits the learning of the inference network when using the wake-phase update (Wake-Wake algorithm).

We refer the reader to [20] for the derivations of the gradients and [9] for an extended review of the RWS algorithms for the training of deep generative models.

The Thermodynamic Variational Objective (TVO) The gradient estimator consists of expressing the marginal log-likelihood $\log p_{\theta}(\mathbf{x})$ using Thermodynamic Integration (TI). Given two unnormalized densities $\tilde{\pi}_0(\mathbf{z})$ and $\tilde{\pi}_1(\mathbf{z})$ and their respective normalizing constants Z_0, Z_1 with $Z_i = \int \tilde{\pi}_i(\mathbf{z}) d\mathbf{z}$ given the unnormalized density $\tilde{\pi}_{\beta}(\mathbf{z}) := \pi_1(\mathbf{z})^{\beta} \pi_0^{1-\beta}(\mathbf{z})$ parameterized by $\beta \in [0, 1]$, and the corresponding normalized density $\pi_{\beta}(\mathbf{z}) = \tilde{\pi}_{\beta}(\mathbf{z}) / \int \tilde{\pi}_{\beta}(\mathbf{z}) d\mathbf{z}$, TI seeks to evaluate the ratio of the normalizing constants using the identity

$$\log Z_1 - \log Z_0 = \int_0^1 \mathbb{E}_{\pi_{\beta}} \left[\frac{d \log \tilde{\pi}_{\beta}(\mathbf{z})}{d\beta} \right] d\beta. \quad (58)$$

[21] connects TI to Variational Inference by setting the base densities as $\tilde{\pi}_0(\mathbf{z}) = q_{\phi}(\mathbf{z}|\mathbf{x})$ and $\tilde{\pi}_1(\mathbf{z}) = p_{\theta}(\mathbf{x}, \mathbf{z})$, which gives the Thermodynamic Variational Identity (TVI):

$$\log p_{\theta}(\mathbf{x}) = \int_0^1 \mathbb{E}_{\pi_{\beta}} \left[\log \frac{p_{\theta}(\mathbf{x}, \mathbf{z})}{q_{\phi}(\mathbf{z}|\mathbf{x})} \right] d\beta. \quad (59)$$

Applying left Riemannian approximation yields the Thermodynamic Variational Objective (TVO):

$$\text{TVO}(\theta, \phi, \mathbf{x}) = \frac{1}{P} \left[\text{ELBO}(\theta, \phi, \mathbf{x}) + \sum_{p=1}^{P-1} \mathbb{E}_{\pi_{\beta_P}} \left[\log \frac{p_{\theta}(\mathbf{x}, \mathbf{z})}{q_{\phi}(\mathbf{z}|\mathbf{x})} \right] \right] \leq \log p_{\theta}(\mathbf{x}). \quad (60)$$

Notably, the integrand $\mathbb{E}_{\pi_{\beta}} \left[\log \frac{p_{\theta}(\mathbf{x}, \mathbf{z})}{q_{\phi}(\mathbf{z}|\mathbf{x})} \right]$ is monotonically increasing, which implies that the TVO is a lower-bound of the marginal log-likelihood.

The TVO allows connecting both Variational Inference and the Wake-Sleep objectives by observing that when using a partition of size $P = 1$, the left Riemannian approximation of the TVI, $\text{TVO}_1^L(\theta, \phi, \mathbf{x}) = \text{ELBO}(\theta, \phi, \mathbf{x})$ and the right Riemannian approximation of the TVI, $\text{TVO}_1^U(\theta, \phi, \mathbf{x})$ is an upper bound of the marginal log-likelihood and equals the objective being maximized in the *wake-phase* for the parameters ϕ of the inference network.

Estimating the gradients of the TVO requires computing the gradient for each of the P expectations $\mathbb{E}_{\pi_{\lambda, \beta}} [f_{\lambda}(\mathbf{z})]$ with respect to a parameter $\lambda := \{\theta, \phi\}$ where $f_{\lambda}(\mathbf{z}) = \log \frac{p_{\theta}(\mathbf{x}, \mathbf{z})}{q_{\phi}(\mathbf{z}|\mathbf{x})}$ and \mathbf{x} is fixed. In

the general case, differentiation through the expectation is not trivial. Therefore the authors propose a score function estimator

$$\nabla_{\lambda} \mathbb{E}_{\pi_{\lambda, \beta}} [f_{\lambda}(\mathbf{z})] = \mathbb{E}_{\pi_{\lambda, \beta}} [\nabla_{\lambda} f_{\lambda}(\mathbf{z})] + \text{Cov}_{\pi_{\lambda, \beta}} [\nabla_{\lambda} \log \tilde{\pi}_{\lambda, \beta}(\mathbf{z}), f_{\lambda}(\mathbf{z})] , \quad (61)$$

where the covariance term can be expressed as

$$\mathbb{E}_{\pi_{\lambda, \beta}} [(f_{\lambda}(\mathbf{z}) - \mathbb{E}_{\pi_{\lambda, \beta}} [f_{\lambda}(\mathbf{z})]) (\nabla_{\lambda} \log \tilde{\pi}_{\lambda, \beta}(\mathbf{z}) - \mathbb{E}_{\pi_{\lambda, \beta}} [\nabla_{\lambda} \log \tilde{\pi}_{\lambda, \beta}(\mathbf{z})])] . \quad (62)$$

The covariance term arises when differentiating an expectation taken over a distribution with an intractable normalizing constant, such as $\pi_{\beta}(\mathbf{z})$ in the TVO. The normalizing constant can be substituted out, resulting in a covariance term involving the tractable un-normalized density $\tilde{\pi}_{\beta}(\mathbf{z})$. Hence, such a covariance term does not usually arise in IWAE due to the derivative of $q_{\phi}(\mathbf{z}|\mathbf{x})$ being available in closed form.

G Gaussian Model

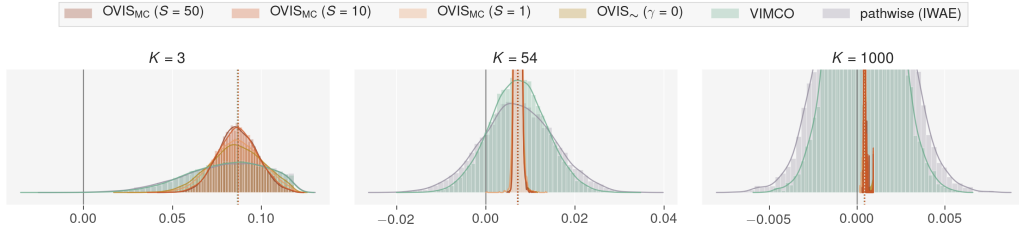


Figure 5: Distribution of the gradients for an arbitrarily chosen component of the parameter \mathbf{b} . The tight control of the variance provided by OVIS allows keeping the distribution of gradients off-center.

Distribution of gradients We report the distributions of the 10^4 MC estimates of the gradient of the first component b_0 of the parameter \mathbf{b} . Figure 5. The pathwise estimator and VIMCO yield estimates which distributions are progressively centered around zero as $K \rightarrow \infty$. The faster decrease of the variance of the gradient estimate for OVIS results in a distribution of gradients that remains off-centered.

Fitting the Gaussian Model We study the relative effect of the different estimators when training the Gaussian toy model from section 6.1. The model is trained for 5.000 epochs using the Adam optimizer with a base learning rate of 10^{-3} and with a batch-size of 100. In Figure 6, we report the L_2 distance from the model parameters A to the optimal parameters A^* , the parameters-average SNR and parameters-average variance of the inference network ($\phi = \{A, \mathbf{b}\}$, $M = \text{card}(\phi)$). We compare OVIS methods with VIMCO, the pathwise IWAE, RWS and the TVO for which we picked a partition size $P = 5$ and $\beta_1 = 10^{-3}$, although no extensive grid search has been implemented to identify the optimal choice for this parameters.

OVIS yields gradient estimates of lower variance than the other methods. The inference network solutions given by OVIS are slightly more accurate than the baseline methods RWS and the TVO, despite being slower to converge. OVIS, RWS and the TVO exhibit gradients with comparable SNR values, which indicate OVIS yield estimate of lower expected value, thus leading to a smaller maximum optimization step-size. Setting $\gamma = 0$ for OVIS_{\sim} results in more accurate solutions than using $\gamma = 1$, this coincides with the measured $\text{ESS} \approx K$.

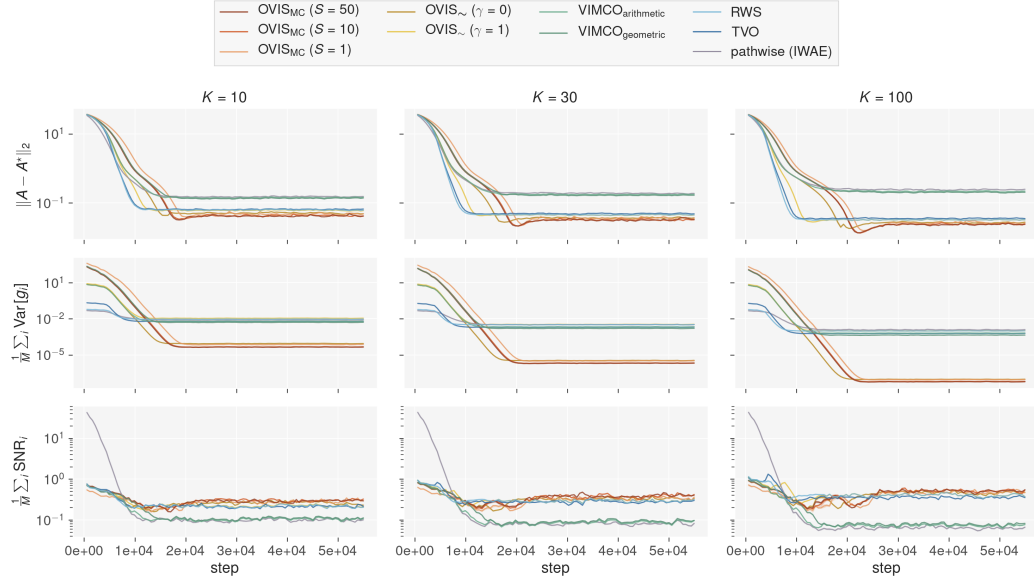


Figure 6: Fitting the Gaussian toy model from section 6.1 and measuring the \mathcal{L}_2 distance with the optimal parameters as well as the variance and the SNR of the gradient estimates. OVIS methods target the optimal parameters A^* of the inference network more accurately than the baseline methods.

H Gaussian Mixture Model

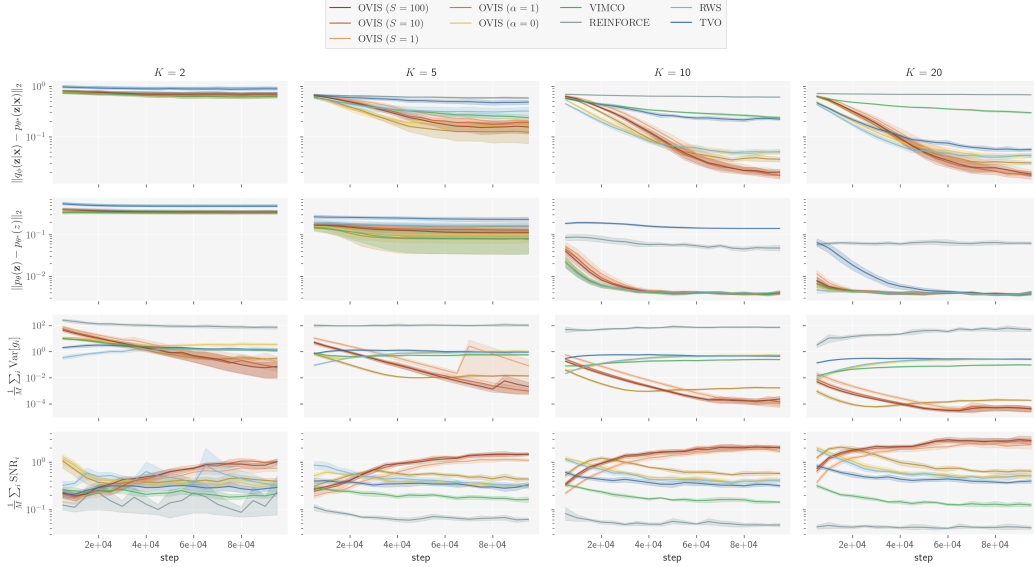


Figure 7: Training curves for the Gaussian Mixture Model for different numbers of particles $K = [2, 5, 10, 20]$ samples averaged over 5 random seeds. The SNR is measured on one mini-batch and averaged over the M parameters of the inference network. In contrast to VIMCO, OVIS estimators all generate gradients with a higher SNR. This results in a more accurate estimate of the true posterior, when compared to VIMCO and the baselines RWS and the TVO.

I Deep Generative Models

I.1 Sigmoid Belief Network

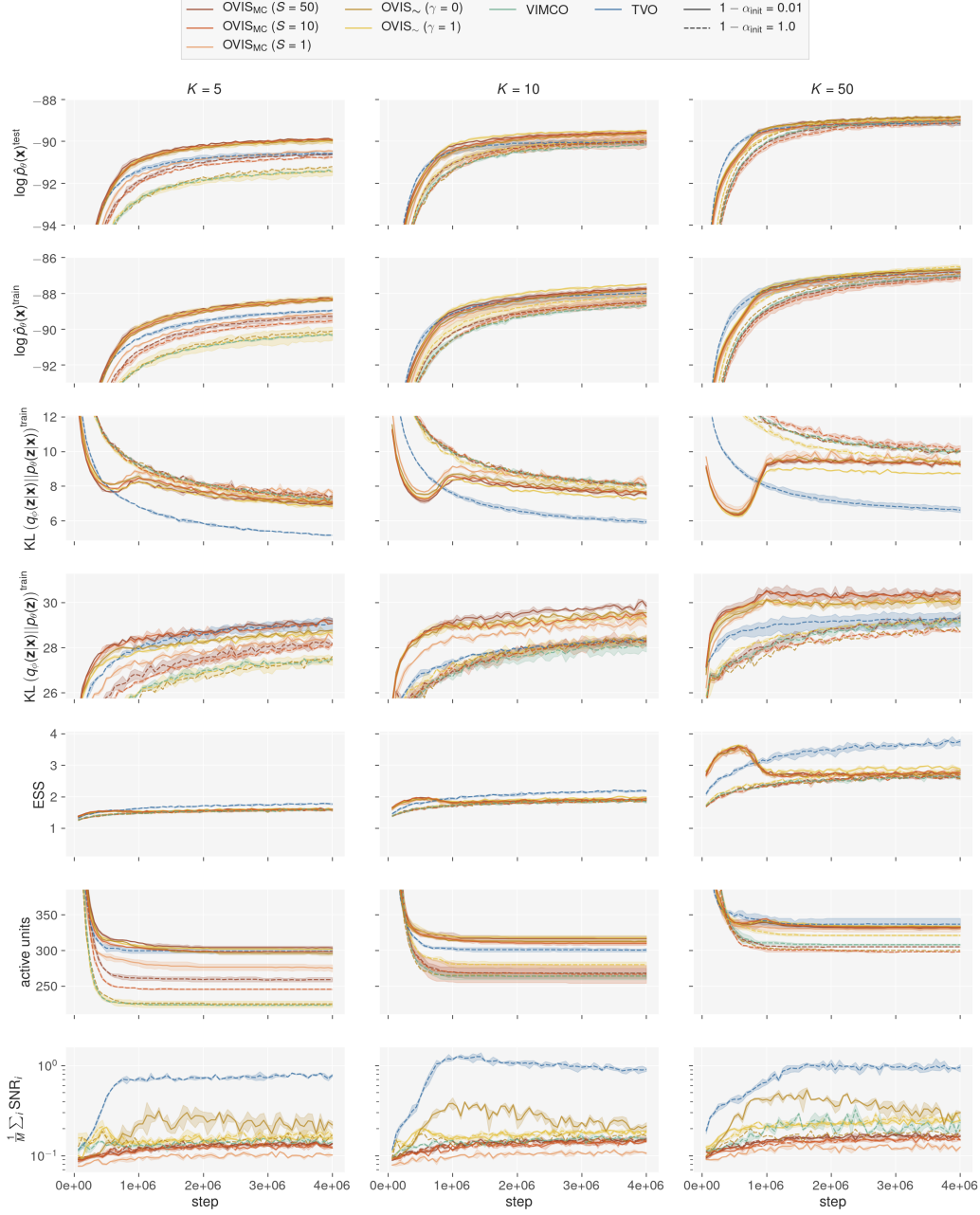


Figure 8: Training curves for the Sigmoid Belief Network using $K = [5, 10, 50]$ particles, using two initial random seeds, with and without using the IWVR bound. The number of active units is evaluated as $\text{AU} = \sum_{d=1}^D \mathbb{1} \{ \text{Cov}_{p(\mathbf{x})} (\mathbb{E}_{q_\phi(z|\mathbf{x})} [z_d]) \geq 0.01 \}$ [22] using 1000 MC samples for each element of a randomly sampled subset of 1000 data points. Warming up the model by optimizing for the IWVR bound with $\alpha > 0$ allows activating a larger number of units and results in models scoring higher training likelihoods.

I.2 Gaussian Variational Autoencoder

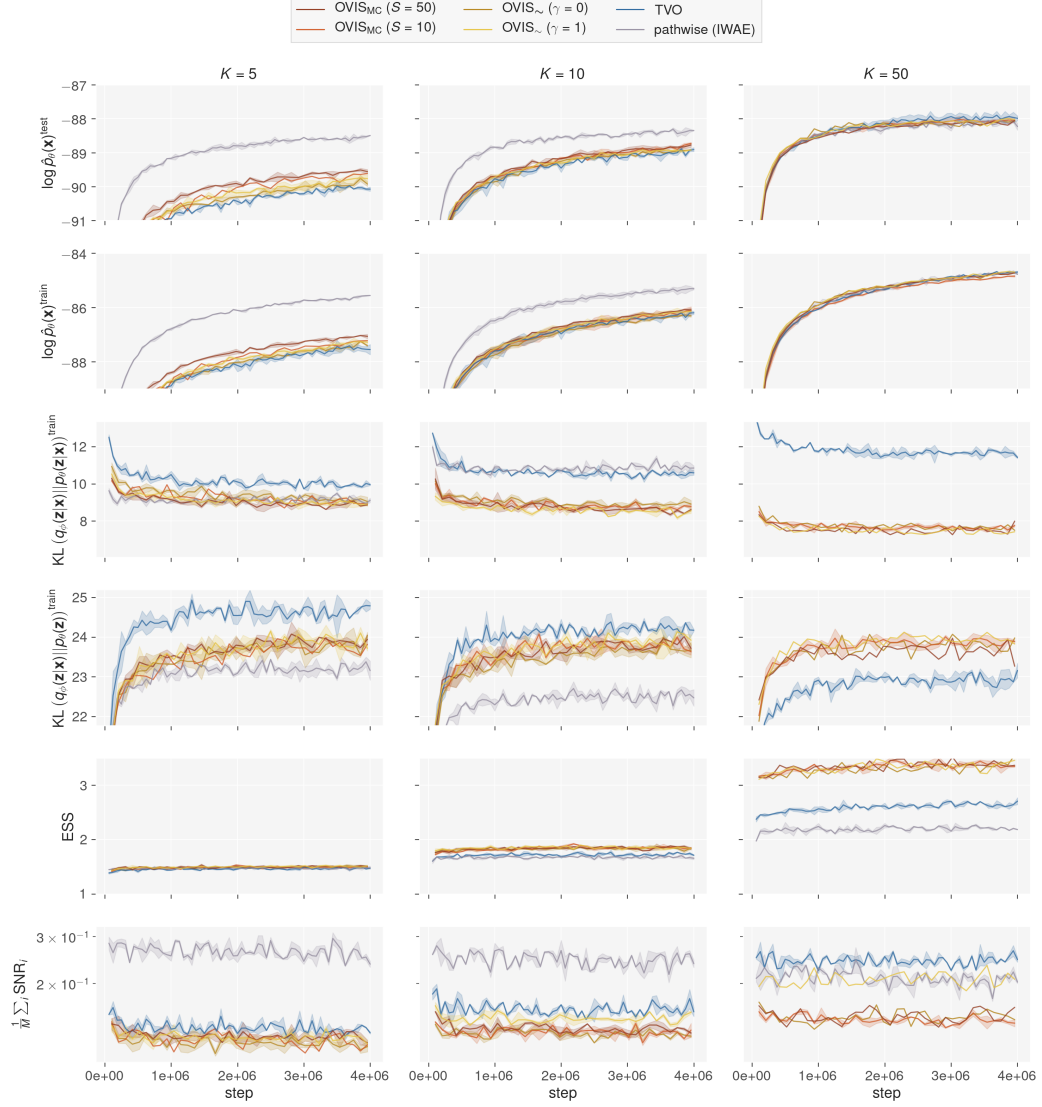


Figure 9: Training curves a Gaussian VAE using $K = [5, 10, 50]$ particles and using two initial random seeds. The OVIS estimators are used in tandem with the IWVR bound with α fixed to 0.3. OVIS for the IWVR bound yields high-quality inference networks, as measured by the divergence $\mathcal{D}_{\text{KL}}(p_\theta(\mathbf{z}|\mathbf{x})||q_\phi(\mathbf{z}|\mathbf{x}))$.